J. Membrane Biol. 178, 185–193 (2000)
DOI: 10.1007/s002320010026

The Journal of
Membrane
Biology



# Charged Residues in Surface-located Loops Influence Voltage Gating of Porin from *Haemophilus influenzae* Type b

**M.A. Arbing[1], D. Dahan[2], D. Boismenu[3], O.A. Mamer[3], J.W. Hanrahan[2], J.W. Coulton[1]**
[1]Department of Microbiology and Immunology, McGill University, 3775 University Street, Montreal, Quebec, Canada, H3A 2B4
[2]Department of Physiology, McGill University, 3655 Promenade Sir-William-Osler, Montreal, Quebec, Canada, H3G IY6
[3]Biomedical Mass Spectrometry Unit, McGill University, 1130 Pine Avenue West, Montreal, Quebec, Canada, H3A 1A3

Received: 11 August 2000/Revised: 8 September 2000

**Abstract.** Porin of *Haemophilus influenzae* type b (341 amino acids; $M_r$ 37782) determines the permeability of the outer membrane to low molecular mass compounds. Purified Hib porin was subjected to chemical modification of lysine residues by succinic anhydride. Electrospray ionization mass spectrometry identified up to 12 modifications per porin molecule. Tryptic digestion of modified Hib porin followed by reverse phase chromatography and matrix assisted laser desorption ionization time-of-flight mass spectrometry mapped the succinylation sites. Most modified lysines are positioned in surface-located loops, numbers 1 and 4 to 7. Succinylated porin was reconstituted into planar lipid bilayers, and biophysical properties were analyzed and compared to Hib porin: there was an increased average single channel conductance compared to Hib porin (1.24+/−0.41 *vs.* 0.85+/−0.40 nanosiemens). The voltage-gating activity of succinylated porin differed considerably from that of Hib porin. The threshold voltage for gating was decreased from 75 to 40 mV. At 80 mV, steady-state conductance for succinylated porin was 50–55% of the instantaneous conductance. Hib porin at 80 mV showed a decrease to 89–91% of the instantaneous current levels. We propose that surface-located lysine residues are determinants of voltage gating for porin of *Haemophilus influenzae* type b.

**Key words:** *Haemophilus influenzae* type b — Porin — Voltage gating — Ion channel

## Introduction

Porins, water-filled proteinaceous channels in the outer membrane (OM) of Gram-negative bacteria, mediate diffusion of hydrophilic solutes between the external environment and the periplasm. Their molecular mass exclusion limit distinguishes this class of membrane proteins. Solutes below the exclusion limit can freely diffuse through the pores while solutes larger than the exclusion limit are restricted in their diffusion. The OM functions selectively as a permeable barrier by excluding noxious compounds such as bile salts, large antibiotics, and detergents from the periplasm. Conversely, porins allow the diffusion of compounds such as amino acids, sugars, and small antibiotics between the external environment and the periplasm (Jap & Walian, 1996; Schirmer, 1998). Porins are also characterized by their voltage gating. They close in response to a voltage above some critical threshold, and the physiological significance of this phenomenon is still unknown (Delcour, 1997; Klebba & Newton, 1998).

Although voltage gating is well documented in vitro, it has yet to be demonstrated in vivo. Sen, Hellman & Nikaido (1988) varied the Donnan potential between 5 and 100 mV (interior negative) across the OM of *E. coli,* but there was no demonstrable change in the uptake of the zwitterionic β-lactam cephaloridine and its subsequent hydrolysis by periplasmic β-lactamase. Because there was no decrease in diffusion of the antibiotic across the OM, Sen et al. (1988) were unable to invoke a role for voltage gating in vivo. However, dela Vega and Delcour (1995) measured the effects of polyamines, which naturally occur as byproducts of amino acid decarboxylation, on two porin-mediated processes in *E. coli:* antibiotic uptake and chemotaxis. The presence of polyamines in the medium inhibited uptake of cephaloridine across the OM and inhibited chemotaxis on swarm plates. They concluded that polyamines inhibited porin-mediated ion flux across the OM. Voltage gating has potential for fine-tuning OM permeability under specific conditions (Samartzidou & Delcour, 1998). Changes of

*Correspondence to:* J.W. Coulton

pH (Todt & McGroarty, 1992) or the presence of membrane derived oligosaccharides (Delcour et al., 1992) in the periplasm have been shown to affect voltage gating.

*Haemophilus influenzae* type b (Hib), an encapsulated Gram-negative bacterium, has six major OM proteins. One of these, OmpP2, displayed channel-forming properties and is the unique porin of this bacterium (Vachon, Lyew & Coulton, 1985). The sequenced *ompP2* gene encodes a polypeptide of 361 amino acids including a signal sequence of 20 amino acids (Munson & Tolan, 1989). After proteolytic cleavage the precursor protein produces a mature protein of 341 amino acids, $M_r$ 37782. The hallmark properties of Hib porin include its molecular mass exclusion limit of 1400 Da (Vachon et al., 1985), a value substantially larger than 600 Da for the porins OmpF, OmpC and PhoE of *Escherichia coli.* Hib porin displays weak cation selectivity (Vachon, Laprade & Coulton, 1986).

Based on the consensus fold of porins, we proposed (Srikumar et al., 1992) a secondary structure model of Hib porin which combined our data on epitope mapping of monoclonal antibody reactivities with flow cytometry of intact bacterial cells. Regions that we predicted by computer-assisted algorithms to form loop 4 and loop 8 were indeed surface-exposed. The region predicted to be loop 3 was not accessible to monoclonal antibodies in flow cytometric assays. We subsequently (Srikumar et al., 1997) mapped the sequence of Hib porin onto the homology derived scaffold from the closest sequence relative, OmpF of *E. coli*, thereby generating a tertiary structure model. Genetic engineering of 6- and 12-amino acid deletions of loops 3 and 4 substantiated our molecular model of Hib porin and its overall structural similarity to other porins.

Biophysical experiments in planar lipid bilayers allow three properties of porins to be measured: ionic selectivity, single channel conductance and voltage gating. Current-voltage curves for porins display ohmic behavior until a threshold voltage is reached. At this threshold voltage the pores begin to close. Whereas ionic selectivity and molecular mass exclusion limits are attributed to atomic features of porin structure, the fundamental mechanism of voltage gating remains elusive. One proposed mechanism is bulk movement of loop 3 (Soares, Björkstén & Tapia, 1995). However tethering loop 3 of OmpF and PhoE porins of *E. coli* to the barrel wall showed no effects on the voltage-gating properties of these proteins (Phale et al., 1997; Eppens et al., 1997). Another possible mechanism might be a subtle repositioning of amino acids in the constriction zone giving blockage of the pore and thereby decreasing conductance (Saxena et al., 1999). We showed (Dahan et al., 1994) that among OMP subtypes of Hib porin, a single mutation (R166Q, subtype 2L) in loop 4 resulted in a decreased threshold voltage for gating. A second variant Hib porin (subtype 6U) that has 10 amino acid substitutions including R166L also showed a decreased threshold for voltage-dependent gating.

This study addresses the hypothesis that positively charged residues determine voltage gating properties. To explore the role of selected amino acids in voltage-gating of Hib porin, we directed attention to surface-accessible charged residues. Studies (Tokunaga, Tokunaga & Nakae, 1981; Przybylski et al., 1996) on functional properties of porins have used chemical modification to alter pore properties. Succinic anhydride covalently modifies solvent-accessible lysine residues, a reaction that results in net charge-reversal. We used chemical modification of lysine residues with succinic anhydride to delineate a subset of the lysine residues (30 in total) of Hib porin that are amenable to chemical modification and that have specific effects on the voltage gating properties of Hib porin. Peptide mapping identified the modified residues and planar lipid bilayer studies assessed the effects of chemical modification on biophysical properties.

## Materials and Methods

### Bacterial Strains and Media

*H. influenzae* type b strain ATCC9795, subtype 1H, was used (Srikumar et al., 1997). Bacteria were grown on chocolate agar plates or in supplemented brain heart infusion broth (Oxoid) as previously described (Srikumar et al., 1997).

### Purification of Hib Porin and Its Succinylation

Hib porin was purified by ion exchange chromatography as previously described (Srikumar et al., 1992) using Zwittergent Z-3,14 (Calbiochem). Purified Hib porin (1 μg/μl) in 50 μl solution containing 50 mM Tris HCl pH 8.0, 200 mM NaCl, 0.1% Zwittergent Z-3,14 was mixed with 10 μl succinic anhydride (SA, 0.2 μg/μl in acetone) giving 1 mol of protein/15 mol SA. After 30 min at 4°C, the reaction was stopped by precipitating the protein with 20 volumes of −20°C cold ethanol and placed at −70°C overnight, a protocol that also removed detergent from the samples. Protein samples were suspended in electrophoresis sample buffer containing 2% SDS, heated for 5 min at 100°C, and run on 10% polyacrylamide gels. Gels were silver stained for protein using a modification of the Morrissey procedure (Morrissey, 1981).

### Mass Spectrometric Analyses of HIB Porin

Protein molecular weights were obtained by resuspending ethanol-precipitated samples of Hib porin or covalently modified porin in formic acid/2-propanol/$H_20$ (1:2:3; v/v) to a final concentration of 250-500 ng/μl. These samples were then mixed 1:1 on the matrix assisted laser desorption ionization time-of-flight mass spectrometry (MALDI-TOF MS; Voyager DE, PerSeptive Biosystems, Framingham, MA) sample plate in saturated solutions of two different matrices: α-cyano-4-hydroxycinnamic acid (Sigma) in 0.3% trifluoroacetic acid (TFA)/

30% acetonitrile; or 3,5-dimethoxy-4-hydroxycinnamic acid (Sigma) in 0.3% TFA/ 50% acetonitrile.

Alternatively, protein samples were resuspended in 40 μl of aqueous 40% methanol/5% acetic acid. Samples were introduced into the mass spectrometer by direct infusion. Spectra were acquired on a Quattro II triple quadrupole equipped with an electrospray source (Micromass; Manchester, UK). Spectra were deconvoluted using Maximum Entropy™ software.

### Tryptic Digestion of HIB Porin and of Covalently Modified Porin

Hib porin and covalently modified porin (200 μg at 3.3 μg/μl) in 50 mM Tris HCl pH 8.0, 200 mM NaCl, 0.1% Zwittergent Z-3,14 were precipitated with 10 volumes of cold ethanol. The dried pellets were resuspended in 100 μl 8 M urea and heated for 30 min at 100°C to denature the protein. The urea concentration was diluted to 0.5 M with the addition of 1500 μl of 25 mM Tris HCl pH 8.0, 100 mM NaCl, and 0.05% Zwittergent Z-3,14. Chemically modified sequencing grade trypsin (Boehringer-Mannheim) in 1 mM HCl (0.25 μg/μl) was added at a ratio of 1:10 (w/w), protease:porin. Digestion proceeded at 37°C for 4 hr. The reaction was stopped with the addition of 1 μg tosyl lysyl chloromethyl ketone (Boehringer-Mannheim). The solution was reduced in volume to approximately 500 μl using a SpeedVac (Savant). Peptides were precipitated with 10 volumes of cold ethanol and stored at −70°C overnight.

### Peptide Mapping

Peptides from Hib porin were analyzed by online LC-ESI-MS using a Hewlett Packard 9010 HPLC coupled to a Quattro II mass spectrometer. Peptides were resuspended in 100 μl mobile phase A (1% acetic acid) for separation on a Vydak C8 column using a linear gradient of mobile phase A and mobile phase B (1% acetic acid in acetonitrile), 5 to 100% B in 30 min. Peptides that were eluted from the column entered directly into the mass spectrometer and were analyzed using cone voltages of 40 or 50 V to select for peptides with different masses. To detect singly- and doubly-charged Hib porin peptides in their most frequently ionized form, a range of 500 to 2500 Da was used. Biolynx software (Micromass) determined the identity of the peptides.

Peptides derived from tryptic digestion of Hib porin and of covalently modified porin were separated by HPLC (Varian 5500 LC). The resulting fragments were analyzed by MALDI-TOF MS. Peptides were resuspended in 100 μl mobile phase A for separation on a Vydak C4 column using a linear gradient of 0.1% trifluoroacetic acid (TFA) (A) and 0.1% TFA, 80% acetonitrile (B), 5 to 100% B in 40 min. Absorbance was measured at 210 nm and 1 ml fractions were collected in siliconized tubes. Fractions were concentrated using a SpeedVac and then analyzed by MALDI-TOF MS. Aliquots of the fractions were mixed 1:1 (v/v) with either of the two matrix solutions (*see above*) directly on the MALDI-TOF plate. Masses were analyzed with the program PROWL (www.prowl.rockefeller.edu) to assign their position within the Hib porin sequence.

### Planar Lipid Bilayer Assays

Planar lipid bilayer studies of single channel conductance were undertaken using a modification of the Mueller and Rudin technique described previously (Srikumar et al., 1997) but with two changes. An operational amplifier (type Axopatch 200B; Axon Instruments, Foster City, CA) was used in a current amplifier configuration to monitor the flow of ions across the membrane. An analog/digital converter and data acquisition software (Digidata 1200A A/D converter and Axoscope 1.0 software; Axon) were used to record the data digitally on a personal computer. More than 200 channel insertions were recorded in each experiment. The amplitude of each channel insertion was measured using the program Axoscope™ and the data arranged as histograms. The average unitary conductance was determined by calculating the geometric mean conductance for the histogram.

Macroscopic conductance measurements were performed (Dahan et al., 1994) with the instrument changes described above. Macroscopic current relaxation curves were well described by single exponentials ($r^2 > 0.92$). Rate constants for pore closure were calculated from least squares fits by using Origin 6.1 software (Microcal, Northampton, MA).

### Abbreviations

The abbreviations used are: OM, outer membrane; Hib, *H. influenzae* type b; SA, succinic anhydride; ESI-MS, electrospray ionization mass spectrometry; MALDI-TOF MS, matrix assisted laser desorption ionization time-of-flight mass spectrometry; nS, nanosiemen(s).

## Results

### Mass Spectrometric Analyses of Hib Porin and of Covalently Modified Porin

Accurate masses of Hib porin and the covalently modified porin sample were obtained by MALDI-TOF MS and ESI MS. MALDI-TOF MS gave a mass of 37800.5 Da for FPLC-purified Hib porin. Confirmation was by ESI mass spectrometry: Hib porin showed one major protein species at 37800.3 Da (Fig. 1*A*). This value is within 0.05% of the value (37782 Da) that was established by DNA sequence analysis of the *ompP2* gene (Munson & Tolan, 1989). After succinylation of Hib porin there was a shift in its electrophoretic mobility upon SDS polyacrylamide gel electrophoresis; compared to the unmodified species, the protein was slightly retarded by a 10% gel. As confirmed by mass spectrometry, there was an increase in the mass of Hib porin following reaction with SA. MALDI-TOF MS analysis gave a broad molecular ion signal that could not be resolved. ESI MS resolved the broad ion peak seen with MALDI-TOF MS. From the deconvoluted ESI mass spectra (Fig. 1*B*), the succinylation reaction resulted in a preparation that we designated SA-porin, varying in mass from 38301.7 Da to 39004.1 Da with approximately 100 Da increments between these two values. Such data reflect the addition of 500 to 1200 Da to Hib porin and therefore correspond to 5 to 12 succinate ($M_r$ 100.08) groups per protein molecule. The highest relative signal intensity of SA-porin was a peak at 38601.6 Da, equivalent to 8 succinate groups on Hib porin.

### Peptide Mapping of Hib Porin and of SA-Porin

To determine the SA modification sites, we established peptide maps for both Hib porin and for SA-

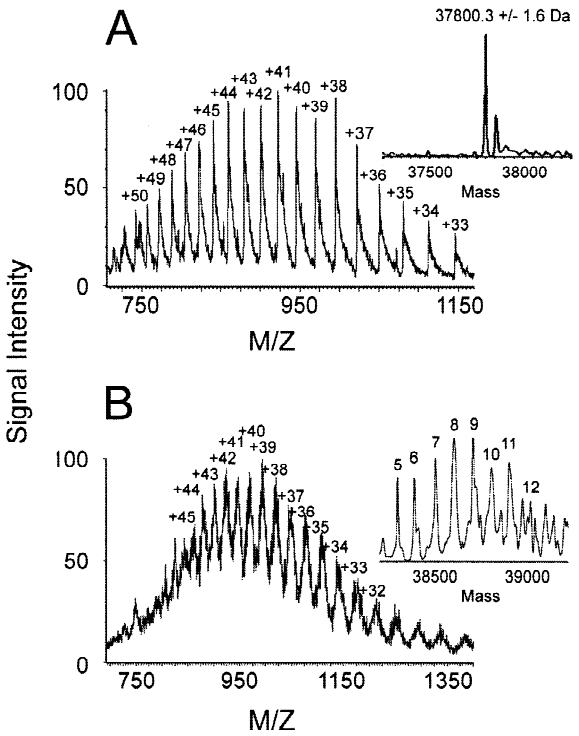


**Fig. 1.** Electrospray mass spectra of Hib porin and SA-porin. (*A*) Mass spectrum of Hib porin. (*B*) Mass spectrum of SA-porin. Insets, deconvoluted mass spectra with predicted masses of the observed ions. Calculated masses are based on charge states in the spectra on the left. In the deconvoluted spectrum of SA-porin the masses of each peak are labeled as the number of modified lysine residues in each protein species. The masses (Da) for these species are as follows: 5, 38303.8 +/− 4.8; 6, 38391.8 +/− 1.7; 7, 38503.3 +/− 2.8; 8, 38601.6 +/− 3.7; 9, 38701.6 +/− 2.2; 10, 38796.8 +/− 5.4; 11, 38896.2 +/− 5.1; 12, 39004.1 +/− 3.8.

porin. Denaturation and digestion of Hib porin with trypsin resulted in near complete cleavage as judged by the absence of protein on SDS-PAGE. Complete fragmentation of Hib porin with trypsin is predicted to produce 46 peptides. Tryptic peptides were separated on reverse phase columns and the fractions were analyzed by mass spectrometry. MALDI-TOF MS analysis showed that some fractions contained more than one peptide. The program PROWL was used to confirm the mass and the identity of Hib porin peptides. MALDI-TOF MS was unable to detect peptides from amino acid sequences containing closely spaced arginine and lysine residues; the peptides fell within the matrix ion peaks. To obtain comprehensive coverage of all Hib porin peptides, samples were eluted from a reverse phase column and infused into an ESI mass spectrometer. The Biolynx software deconvoluted the mass spectra, confirmed that most peaks contained more than one peptide, accurately assessed their molecular masses, and established their position in the amino acid sequence of Hib porin. Analysis of peptide masses resulting from MS mapping revealed that complete digestion of Hib porin did not occur. Many partial fragments were detected. The combination of mass spectrometry technologies generated a reference map (Table 1) that identifies 24 peptides and accounts for 82% of the primary amino acid sequence of Hib porin.

When SA-porin was analyzed, lysine-modified residues were no longer susceptible to cleavage by trypsin and so only 19 peptides were detected by MALDI-TOF MS. Their masses reflected the absence of potential cleavage sites and they increased by the mass of a succinate group per fragment per modified lysine residue. Reverse phase HPLC separated the tryptic peptides and MALDI-TOF MS analysis was performed on all fractions. Table 2 identifies the 19 peptides and they correspond to 92% of the primary amino acid sequence. Using this strategy, 12 succinylation sites were routinely observed: 11 lysines plus the amino terminal alanine residue. Some lysine residues (K32, K161, K165, K206, K214, and K253) were modified preferentially as assessed by an absence of the unmodified constituent peptides in MALDI-TOF MS analysis. Lysines K48, K170, K248, K250, K287, and alanine 1 were subject to lesser modification as indicated by the presence of both SA-modified and unmodified peptides. Experimental and theoretical masses of peptides are reported in Table 2. Three peptides were not isolated, corresponding to the amino acids 255-276, 277-279 and 316-317 in the Hib porin amino acid sequence. The hydrophobicity of the largest peptide (255-276) may have resulted in its decreased solubility and thus it would be refractory to identification. Alternatively, nonspecific adsorption to reaction vessels may account for peptide loss during sample preparation.

## Electrophysiological Characterization of SA-Porin

To test their channel-forming properties, Hib porin and SA-porin were reconstituted into planar lipid bilayers. More than 200 single channel insertion events were measured for both samples. The histograms in Fig. 2 display the distribution of open channel amplitudes. Hib porin showed conductance steps between 0.10 and 2.10 nS (Fig. 2*A*). The geometric mean conductance from the Hib porin histogram was 0.85 +/− 0.40 nS, a feature of Hib porin that has been reported previously by our laboratory (Srikumar et al., 1997). When three different preparations of Hib porin were analyzed for single channel conductance, the distributions of conductance steps in their respective histograms were identical. There was also little variation among triplicate preparations of SA-porin. As our FPLC-purified Hib porin preparations demonstrate no evidence of trimers under nondenaturing PAGE conditions, we consider this value to represent the

**Table 1.** Tryptic fragments from digestion of Hib porin identified by MALDI-TOF mass spectrometry analysis of HPLC fractions and LC-ESI-MS of Hib porin digests

| Residues | Calculated mass +H | Measured mass | Peptide sequence |
|---|---|---|---|
| 1–16 | 1691.8 | 1692.4 | AVVYNNEGTNVELGGR |
| 17–32 | 1746.9 | 1746.8 | LSIIAEQSNSTVDNQK |
| 33–39 | 809.4 | 808.7 | QQHGALR |
| 40–44 | 561.3 | 561.9 | NQGSR |
| 45–48 | 544.3 | 542.9 | FHIK |
| 49–66 | 2046.9 | 2047.9 | ATHNFGDGFYAQGYLETR |
| 67–94 | 3028.3 | 3029.1 | FVTKASENGSDNFGDITSKYAYVTLGNK |
| 95–100 | 650.4 | 650.0 | AFGEVK |
| 101–103 | 345.2 | 343.6 | LGR |
| 104–105 | 218.2 | 217.6 | AK |
| 106–117 | 1220.6 | 1220.7 | TIADGITSAEDK |
| 141–165 | 2616.0 | 2616.0 | GIDGLVLGANYLLAQKREGAKGENK |
| 166–170 | 629.7 | 630.2 | RPNDK |
| 171–175 | 531.3 | 530.0 | AGEVR |
| 189–197 | 1008.5 | 1007.6 | YDANDIVAK |
| 198–202 | 579.3 | 578.0 | IAYGR |
| 203–227 | 2943.2 | 2945.3 | TNYKYNESDEHKQQLNGVLATLGYR |
| 228–243 | 1684.9 | 1684.5 | FSDLGLLVSLDSGYAK |
| 246–248 | 424.2 | 423.1 | NYK |
| 249–253 | 654.8 | 655.4 | IKHEK |
| 255–276 | 2650.0 | 2653.9 | YFVSPGFQYELMEDTNVYGNFK |
| 280–287 | 863.4 | 861.8 | TSVDQGEK |
| 304–315 | 1397.7 | 1396.8 | QLLTYIEGAYAR |
| 318–341 | 2613.4 | 2617.2 | TTETGKGVKTEKEKSVGVGLRVYF |

Calculated peptide mass was determined by amino acid sequence analysis of Hib porin using the programs Biolynx and PROWL.

unitary conductance of a Hib porin monomer. SA-porin also formed stable pores, although there was some increase in the open channel noise of SA-porin when compared to Hib porin (Fig. 2*B*). The unitary conductance of SA-porin suggests that they too insert into the membrane as monomers, and this insertion apparently occurred more slowly with the modified porins than with Hib porin. SA-porin also showed a distribution of conductance steps that was shifted to higher conductance values compared to Hib porin. The majority of steps were found between 0.9 and 1.5 nS and fewer than 5% of conductance steps occurred above 2.1 nS. The geometric mean conductance of SA-porin was 1.24 +/− 0.41 nS, significantly higher than that of Hib porin (0.85 +/− 0.4 nS). As determined by a z-test of independent means, the increase in geometric mean conductance of SA-porin *vs.* Hib porin was determined to be statistically significant at the $P < 0.0001$ level.

The voltage gating of Hib porin and SA-porin was compared by determining the threshold at which macroscopic conductance spontaneously declines following a voltage step. The threshold is defined as the voltage above which the steady-state current-voltage relationship becomes nonlinear and the current rapidly relaxes to a lower value. The membrane was allowed to stabilize after porin insertions. Bilayers typically contained approximately 50 channels. As membrane breakage may occur when obtaining measurements, experiments were begun with a holding potential of 20 mV after porin insertion had stabilized. The current amplitudes at this holding potential were used to normalize data obtained for experiments with Hib porin and SA-porin. When steady state current levels had been reached, voltage steps from a holding potential of 0 mV were applied over a range of −80 to +80 mV and terminated after a steady-state current level was reached (1–3 min). Normalized instantaneous and steady state current-voltage relations with standard deviations are shown for both Hib porin (Fig. 3*A*) and SA-porin (Fig. 3*C*). When the voltage exceeded +/− 75 mV, current mediated by Hib porin relaxed to a steady-state level that was approximately 9–11% lower than the instantaneous current. The *I/V* relationship was linear below the threshold voltage, as in our previous study (Dahan et al., 1994). The macroscopic conductance of SA-porin was more voltage dependent than for Hib porin, with threshold voltage decreasing to approximately 40 mV for SA-porin *vs.* 75 mV for Hib porin. Both the magnitude and rate of current decay were also altered (Figs. 3*B, D*). Whereas at 80 mV, Hib porin current decayed to a steady-state current 10.5% +/− 2.9 ($n = 3$) lower than the instantaneous current level, SA-porin current decayed to a steady state

**Table 2.** Tryptic fragments and succinylated lysine residues as determined by MALDI-TOF MS analysis of HPLC fractionated peptides of SA-porin.

| Residues | Calculated mass + H | Measured mass | Peptide sequence | Modified residues |
|---|---|---|---|---|
| 1–16 | 1792.9 | 1793.7 | AVVYNNEGTNVELGGR | N-terminus |
| 17–44 | 3180.1 | 3181.4 | LSIIAEQSNSTVDNQKQQHGALRNQGSR | K32 |
| 45–66 | 2673.9 | 2670.5 | FHIKATHNFGDGFYAQGYLETR | K48 |
| 67–94 | 3028.3 | 3026.7 | FVTKASENGSDNFGDITSKYAYVTLGNK | |
| 95–117 | 2378.7 | 2376.1 | AFGEVKLGRAKTIADGITSAEDK | |
| 118–156 | 4167.7 | 4167.2 | EYGVLNNSDYIPTSGNTVGYTFKGIDGLVLGANYLLAQK | |
| 141–165 | 2616.0 | 2615.3 | GIDGLVLGANYLLAQKREGAKGENK | |
| 158–175 | 2256.4 | 2253.6 | EGAKGENKRPNDKAGEVR | K161, K165, K170 |
| 171–202 | 3376.8 | 3379.7 | AGEVRIGEINNGIQVGAKYDANDIVAKIAYGR | |
| 203–227 | 3143.4 | 3136.5 | TNYKYNESDEHKQQLNGVLATLGYR | K206, K214 |
| 228–243 | 1685.9 | 1685.3 | FSDLGLLVSLDSGYAK | |
| 244–253 | 1289.5 | 1288.3 | TKNYKIKHEK | |
| 246–254 | 1516.7 | 1515.9 | NYKIKHEKR | K248, K250, K253 |
| 249–254 | 1011.1 | 1010.4 | IKHEKR | K250, K253 |
| 251–254 | 669.7 | 669.4 | HEKR | K253 |
| 280–289 | 1221.3 | 1221.0 | TSVDQGEKTR | K287 |
| 290–315 | 3001.5 | 3000.7 | EQAVLFGVDHKLHKQLLTYIEGAYAR | |
| 318–341 | 2615.0 | 2615.3 | TTETGKGVKTEKEKSVGVGLRVYF | |

Calculated peptide mass was determined by amino acid sequence analysis of Hib porin using the program PROWL.

current that was 46.9% +/− 5.0 ($n = 6$) lower than the instantaneous current at the same test voltage (80 mV). Channel inactivation appeared as a series of small steps occurring at 1–5 sec intervals. The conductance amplitude of most of these closing steps fell between 1.0 and 1.5 nS for SA-porin. Voltage gating of SA-porin was also enhanced at negative potentials. Currents decayed by 38.5% +/− 3.5 ($n = 3$) at a holding potential of −80 mV compared to Hib porin currents, which decayed only 8.9% +/− 1.5 ($n = 3$) from the instantaneous current at voltages beyond −75 mV. The decay was fully reversible for both Hib porin and SA-porin. Identical instantaneous conductances were obtained when the applied voltage was turned off and then reapplied.

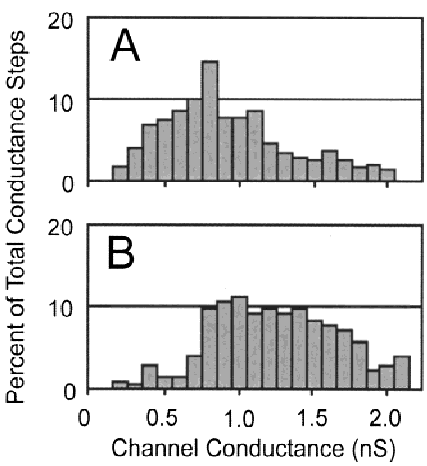


**Fig. 2.** Comparison of channel conductances of Hib porin (*A*) and SA-porin (*B*) in planar lipid bilayers. The porins were diluted with 10 mM Tris pH 8.0 to 1 ng/μl. Five μl of this material was added to the *cis* side of the bilayer chamber containing 1 M KCl so that the final porin concentration was approximately 1 ng/ml. The total number of conductance steps analyzed was as follows: (*A*) 249; (*B*) 265.

We compared the rate of entry from the open state into the inactivated state by fitting macroscopic current relaxation curves with an exponential function to determine the time constant (τ) of the process. The mean time constant for Hib porin at +80 mV was 103.3 +/− 41.6 sec ($n = 3$), indicating that Hib porin pore closure is a relatively slow process. By contrast, the time constant of SA-porin at the same holding potential was 2.8 +/− 0.9 sec ($n = 4$). It was not possible to make reliable fits at other test voltages.

## Discussion

Different loops of bacterial porins apparently play specific roles in pore functions. Loop 3 contributes to the geometry of the constriction zone, thereby limiting the size of compounds that diffuse freely through the porin channel (Jap & Walian, 1996). Loop 2, the latching loop in *E. coli* OmpF, contacts the adjacent monomer in an OmpF homotrimer, forming ionic and hydrogen bonds with the neighboring channel. These bonds are important for trimer stability (Phale et al., 1998). Because we are specifically interested in the role of the extracellular loops of Hib porin that influence voltage gating, our

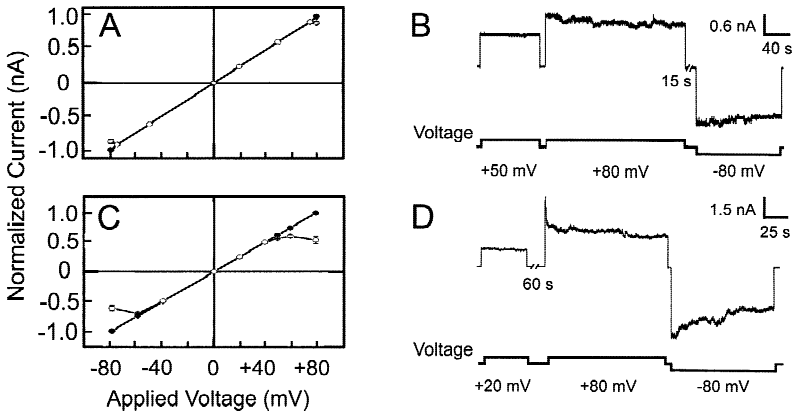


**Fig. 3.** Current-voltage curves of planar lipid bilayers containing Hib porin (*A*) or SA porin (*C*). Closed circles represent the instantaneous current through membranes while open circles represent steady-state current reached 1 to 2 min after application of the test voltage. Each symbol represents the values (+/− SD) from 3–6 experiments. Error bars may lie within the thickness of the symbols. Porin samples were added to the *cis* side of the chamber after forming bilayers to allow porin insertions from only one side of the chamber. (*B*) and (*D*) show current tracings for Hib porin and SA-porin, respectively. Breaks in the data between voltage steps are represented by slanted lines with the duration shown below. Voltage steps were applied as indicated in the lower tracings.

strategy was to use chemical modification to target solvent accessible lysine residues of Hib porin and to assess the effects of lysine residues on the voltage gating of Hib porin.

Given our homology model for Hib porin and a total of 30 lysines in the protein, we position 14 lysines in the lumen of the pore (Srikumar et al., 1997). Of these 14, only K48 was found to be SA-modified. In the homology model residue 48 extends inwards from β strand 2 and is between the constriction zone and the periplasmic side. This modification by SA reflects the restricted solvent accessibility of lysine residues within the lumen of the pore. Strikingly, peptide mapping determined three (K161, K165, K170) of the four lysines in loop 4 (Fig. 4) to be SA-modified. Besides SA modification of the amino terminus, the remaining SA modifications are positioned in our homology model in loop 1 (K32), loop 5 (K206, K214), loop 6 (K248, K250, K253), and loop 7 (K287). Some flexibility of extracellular loops may allow their increased accessibility to the modifying reagent. Tertiary complexes between porin molecules in solution could further limit access of the modifying reagent to lysine residues.

Compared to Hib porin (0.85 +/−0.40 nS), the average single channel conductance (1.24 +/– 0.41 nS) of SA-porin is increased. One might expect the addition of a succinate group in the barrel lumen to block the pore and result in decreased conductance. Using crystallographic data for *Paracoccus denitrificans* porin, Saxena et al. (1999) mutated an aspartate residue located in the lumen to a tryptophan. They noted that the mutation resulted in an increased single channel conductance. Despite the addition of a bulky succinate group in the lumen of Hib porin, we also found increased conductance of our SA-porin, a phenomenon that may be attributed to conformational changes in the extracellular loops. Previous studies (Srikumar et al., 1997) in our laboratory have shown that deletions of 6- and 12- amino acids in the predicted loop 4 gave increases in the single channel conductance of Hib porin. We proposed that loop 4 extends over the lumen of the pore and thus limits ions from permeating into the pore. By introducing negative charges into the extracellular loops, electrostatic repulsion may reorient the loops in SA-porin relative to their positions in Hib porin. Electrostatic repulsion could also open the pore allowing increased ion access

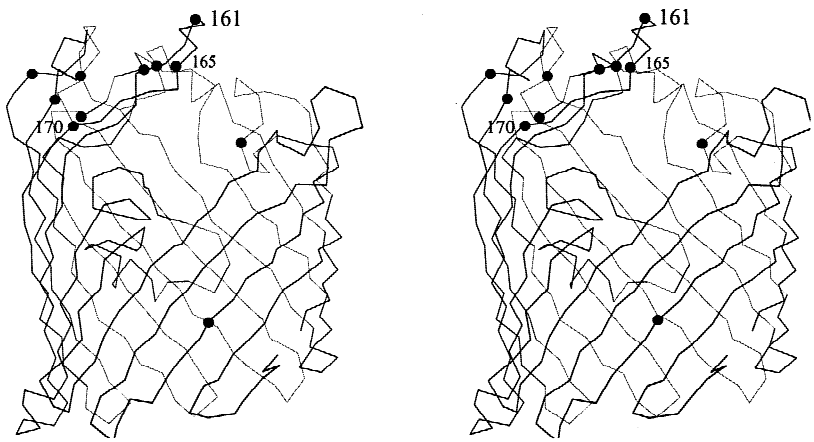


**Fig. 4.** Cα trace (stereo) model of Hib porin generated by homology modeling using the Swiss-Model server and improved manually (Srikumar, 1997). The locations of the SA-modified lysines are indicated by black spheres. The modified lysine residues K161, K165, K170 located in loop 4 are labeled.

and higher single channel conductivities. We observed that the threshold voltage for gating of SA-porin is substantially decreased compared to Hib porin. Using covalent modification, we converted a voltage-independent pore into a channel that had a low threshold voltage for gating. That value at positive polarity became 40 mV *vs.* 75 mV of Hib porin and steady-state current levels decreased to 50–55% of the instantaneous current level. We previously observed this phenomenon (Dahan et al., 1994) with the loss of positive charge (R166Q, in porin subtype 2L) in the proposed loop 4. Hib porin, subtype 6U, which has 10 amino acid substitutions including R166L, also displayed a lower threshold voltage for gating. Gating of SA-porin was increased at negative polarity *vs.* Hib porin. Above an applied voltage of −40 mV the channel began to close. The extent of gating at negative polarity was less severe than at positive potentials and may reflect an asymmetric distribution of modified lysines. Loss of surface-exposed positive charges therefore appears to play a role in the gating of Hib porin. SA-porin had an overall decrease in net charge because modification of each lysine residue resulted in a decrease of 2 in charge. The majority of the modified lysines are positioned in surface-exposed loops and they are clustered in the proposed loop 4.

A recent study suggests an alternative method by which pores may be gated. Müller and Engel (1999) used atomic force microscopy to establish closure of *E. coli* OmpF pores. By generating Nernst potentials exceeding the threshold voltage or by lowering the pH, they visualized a decrease from 13 to 6 Å in the height of the extracellular domains corresponding to the loops of OmpF. Upon returning experimental conditions to physiological pH, or by lowering the applied voltage to below the threshold voltage, the loops reverted to their original conformation. They attributed the conformational change in the extracellular domains of OmpF to the collapse of the loops into the vestibule of the pore. Pore closure could result. These data correlate with the voltage gating of porins and β barrel toxins that have extracellular loops as common structural features. The results of Müller and Engel are therefore in concordance with this study and with our previous results (Dahan et al., 1994).

The mechanism that the pore uses to sense an external voltage source has not been established. Recent studies indicate that positive charges act as sensors in anion-specific pores and that negative charges act as the voltage sensors in cation-selective pores (Van Gelder et al., 1997; Saxena et al., 1999). Van Gelder et al. (1997) postulated that substitution of charged residues in the pore constriction disturbs the transverse electric field that lies horizontally across the pore lumen thereby disrupting ion flow through the pore. That our studies have induced a similar effect by introducing negative charges into the extracellular loops and one channel site suggests that more than disruption of the transverse electric field in the barrel lumen is responsible for the breakdown of ion flux.

We addressed the hypothesis that positively charged residues determine voltage-gating properties. By directing attention to surface-accessible charged residues and reversing the charge of these residues, we induced substantial voltage-gating behavior in what was nominally a voltage independent channel. Our studies show loss of positive charges in the extracellular loops of porin subtypes and SA-porin results in a decreased threshold voltage in comparison to Hib porin. Different Hib porin subtypes (Dahan et al., 1994) and now SA-porin demonstrate voltage gating because of the loss of positive charges in extracellular loops. We conclude that selected positively charged residues in the extracellular loops play a central role in the gating of Hib porin.

This work was supported in part by a grant (MT-14133 to J.W.C.) from the Medical Research Council, Canada. MALDI-TOF MS experiments were performed at the Sheldon Biotechnology Center (SBC), McGill University. SBC is supported by a Multi-user equipment and maintenance grant from Medical Research Council, Canada. The authors thank H.P.J. Bennett for many helpful discussions on peptide purification and MALDI-TOF MS; and K. Diederichs for assistance with the stereofigure. We appreciate critical reviews of the manuscript by F.F. Arhin and M. Bonhivers as well as editing by J.A. Kashul.

## References

Dahan, D., Vachon, V., Laprade, R., Coulton, J.W. 1994. Voltage gating of porins from *Haemophilus influenzae* type b. *Biochim. Biophys. Acta* **1189:**204–211

dela Vega, A.L., Delcour, A.H. 1995. Caderine induces closing of *E. coli* porins. *EMBO J.* **14:**6058–6065

Delcour, A.H. 1997. Function and modulation of bacterial porins: insights from electrophysiology. *FEMS Micro. Lett.* **151:**115–123

Delcour, A.H., Adler, J., Kung, C., Martinac, B. 1992. Membrane-derived oligosaccharides (MDOs) promote closing of an *E. coli* porin channel. *FEBS Lett.* **304:**216–220

Eppens, E.F., Saint, N., Van Gelder, P., van Boxtel, R., Tommassen, J. 1997. Role of the constriction loop in the gating of outer membrane porin PhoE of *Escherichia coli. FEBS Lett.* **415:**317–320

Jap, B.K., Walian, P.J. 1996. Structure and functional mechanism of porins. *Physiol. Rev.* **76:**1073–1088

Klebba, P.E., Newton, S.M.C. 1998. Mechanisms of solute transport through outer membrane porins: burning down the house. *Curr. Opin. Microbiol.* **1:**238–248

Morrissey, J.H. 1981. Silver stain for proteins in polyacrylamide gels: a modified procedure with enhanced uniform sensitivity. *Anal. Biochem.* **117:**117–310

Müller, D.J., Engel, A. 1999. Voltage and pH-induced channel closure of porin OmpF visualized by atomic force microscopy. *J. Mol. Biol.* **285:**1347–51

Munson, R., Jr., Tolan, R.W. Jr. 1989. Molecular cloning, expression, and primary sequence of outer membrane protein P2 of *Haemophilus influenzae* type b. *Infect. Immun.* **57:**88–94

Phale, P.S., Philippsen, A., Kiefhaber, T., Koebnik, R., Phale, V.P., Schirmer, T., Rosenbusch, J.P. 1998. Stability of trimeric OmpF porin: the contributions of the latching loop L2. *Biochemistry* **37:**15663–15670

Phale, P.S., Schirmer, T., Prilipov, A., Lou, K-L., Hardmeyer, A., Rosenbusch, J.P. 1997. Voltage gating of *Escherichia coli* porin channels: role of the constriction loop. *Proc. Natl. Acad. Sci. USA* **94:**6741–6745

Przybylski, M., Glocker, M.O., Nestel, U., Schnaible, V., Blüggel, M., Diederichs, K., Weckesser, J., Schad, M., Schmid, A., Welte, W., Benz, R. 1996. X-ray crystallographic and mass spectrometric structure determination and functional characterization of succinylated porin from *Rhodobacter capsulatus:* implications for ion selectivity and single-channel conductance. *Prot. Sci.* **5:**1477-1489

Samartzidou, H., Delcour, A.H. 1998. *E. coli* PhoE porin has an opposite voltage-dependence to the homologous OmpF. *EMBO* **17:**93–100

Saxena, K., Drosou, V., Maier, E., Benz, R., Ludwig, B. 1999. Ion selectivity reversal and induction of voltage gating by site-directed mutations in the *Paracoccus denitrificans* porin. *Biochemistry* **38:**2206–2212

Schirmer, T. 1998. General and specific porins from bacterial outer membranes. *J. Struct. Biol.* **121:**101–109

Sen, K., Hellman, J., Nikaido, H. 1988. Porin channels in intact cells of *Escherichia coli* are not affected by Donnan potentials across the outer membrane. *J. Biol. Chem.* **263:**1182-1187

Soares, C.M., Björkstén, J., Tapia, O. 1995. L3 loop-mediated mechanisms of pore closing in porin: a molecular dynamics perturbation approach. *Protein Engineering* **8:**5–12

Srikumar, R., Chin, A.C., Vachon, V., Richardson, C.D., Ratcliffe, M.J.H., Saarinen, L., Käyhty H., Mäkelä, P.H., Coulton, J.W. 1992. Monoclonal antibodies specific to porin of *Haemophilus influenzae* type b: localization of their cognate epitopes and tests of their biological activities. *Mol. Microbiol.* **6:**665–676

Srikumar, R., Dahan, D., Arhin, F.F., Tawa, P., Diederichs, K., Coulton, J.W. 1997. Porins of *Haemophilus influenzae* type b mutated in loop 3 and in loop 4. *J. Biol. Chem.* **272:**13614–13621

Srikumar, R., Dahan, D., Gras, M.F., Ratcliffe, M.J.H., van Alphen, L., Coulton, J.W. 1992. Antigenic sites on porin of *Haemophilus influenzae* type b: mapping with synthetic peptides and evaluation of structure predictions. *J Bacteriol.* **174:**4007–4016

Todt, J.C., McGroarty, E.J. 1992. Acid pH decreases OmpF and OmpC channel size in vivo. *Biochem. Biophys. Res. Commun.* **189:**1498–1502

Tokunaga; H., Tokunaga, M., Nakae, T. 1981. Permeability properties of chemically modified porin trimers from *Escherichia coli* B. *J. Biol. Chem.* **256:**8024–8029

Vachon, V., Laprade, R., Coulton, J.W. 1986. Properties of the porin of *Haemophilus influenzae* type b in planar lipid bilayer membranes. *Biochim. Biophys. Acta* **861:**74–82

Vachon, V., Lyew, D.J., Coulton, J.W. 1985. Transmembrane permeability channels across the outer membrane of *Haemophilus influenzae* type b. *J. Bacteriol.* **162:**918–924

Van Gelder, P., Saint, N., Phale, P., Eppens, E., Prilipov, A., van Boxtel, R., Rosenbusch, J.P., Tommassen, J. 1997. Voltage sensing in the PhoE and OmpF outer membrane porins of *Escherichia coli:* role of charged residues. *J. Mol. Biol.* **269:**468–472